

**X-RAY STRUCTURAL STUDIES OF SOME  
NATURAL PRODUCTS FROM  
*RAUWENHOFFIA SIAMENSIS* SCHEFF.,  
*PRISMATOMERIS MALAYANA* RIDL.,  
*CRATOXYLUM FORMOSUM* SSP.  
*PRUNIFOLUM* AND *ANDROGRAPHIS*  
*PANICULATA* NEES PLANTS**

**NG SHEA LIN**

**UNIVERSITI SAINS MALAYSIA  
2008**

## **ACKNOWLEDGEMENT**

First of all, I would like to offer my most grateful thanks to my supervisor, Dr. Abdul Razak Ibrahim and co-supervisor, Professor Fun Hoong Kun for their guidance, valuable advice, encouragement, patience and understanding throughout my research. I am also deeply grateful to my external supervisor, Dr. Suchada Chantrapromma and researchers from Thailand and Universiti Putra Malaysia for their help, useful advice and encouragement.

I would also like to thank the Malaysian Government and Universiti Sains Malaysia for the post of research officer through the Scientific Advancement Grant Allocation (SAGA) grant no. 304/PFIZIK/653003/A118, Science Fund grant No. 305 / PFIZIK / 613312 and the USM short-term grant no. 304/PFIZIK/635028 which give me the opportunity to carry out my research. I am grateful to the School of Physics, Universiti Sains Malaysia for allowing me to use the equipment in the X-ray Crystallography Laboratory for my research. Also, my special thanks to the Institut Pengajian Siswazah (IPS), Universiti Sains Malaysia for the opportunity to further my masters degree.

Special thanks to Encik K. Karunakaran for the support and assistance during my research in the X-ray Crystallography Laboratory. I am also grateful to all of my fellow friends for their moral support.

Finally, I would like to thank all my family members, my father Ng Tiang Nyo, my mother Tan Chin Kim, my brother Ng Heng Leong and my sister Ng Shue Ki for their valuable comments, encouragement and understanding.

## TABLE OF CONTENTS

	Page
Acknowledgements	ii
Table of Contents	iv
List of Tables	ix
List of Figures	xi
List of Plates	xiv
List of Abbreviations	xv
Abstrak	xvi
Abstract	xix
<b>CHAPTER 1          INTRODUCTION</b>	
1.1    Preliminary	1
1.2    X-ray Crystallography	1
1.3    Generation of X-Ray	1
1.4    X-Ray Diffraction	4
1.5    Reciprocal Lattice	7
1.6    Ewald Sphere	9
1.7    Natural Product	11
1.7.1   1-(2,4-Dihydroxy-6-methoxyphenyl)-3-(4-methoxyphenyl) propan-1-one	14
1.7.2   1-3-Dihydroxy-2-methyl-9,10-anthraquinone	14
1.7.3   12-(1,1-Dimethyl-2-propenyl)-5,9,10-trihydroxy-2,2- dimethyl-2 <i>H</i> ,6 <i>H</i> -pyrano[3,2- <i>b</i> ]xanthen-6-one	15
1.7.4   3,19-(2-Bromobenzylidene)andrographolide	15
1.7.5   3,19-(2,6-Dimethoxybenzylidene)andrographolide	16

1.8	Objective	17
1.9	Thesis Overview	18
<b>CHAPTER 2        X-RAY STRUCTURE ANALYSIS</b>		
2.1	Argand Diagram	19
2.2	Combination of N Waves	21
2.3	Phase Difference	22
2.4	The Atomic Scattering Factor	23
2.5	Structure Factor	25
2.6	Friedel's Law	28
2.7	Limiting Conditions and Systematic Absences	30
2.8	Electron Density Distribution	33
2.9	Patterson Method (Heavy Atom Method)	35
2.9.1	Patterson Function	35
2.9.2	One-Dimensional Patterson Function	36
2.9.3	Three-Dimensional Patterson Function	38
2.9.4	Partial Fourier Synthesis	39
2.9.5	Successive Fourier Refinement	41
2.9.6	Sharpened Patterson Function	42
2.9.7	Difference-Fourier Synthesis	43
2.10	Direct Methods	45
2.10.1	Harker and Kasper Inequalities	45
2.10.2	Sayre Equation	46
2.10.3	$\sum_2$ Relation	47
2.10.4	Tangent Formula	49

2.11	Data Reduction	49
2.11.1	Lorentz and Polarization Corrections	51
2.11.2	Absorption Correction	52
2.12	Structure Solution	55
2.13	Structure Refinement	56
2.13.1	Principle of Least-Squares Refinement	56
2.13.2	Weights	57
2.13.3	Refinement Statistics	58
2.14	Ring Conformation	59
 <b>CHAPTER 3            METHODOLOGY</b>		
3.1	Introduction	63
3.2	Single Crystal Diffractometer System BRUKER APEX II SMART CCD Area Detector	64
3.3	SMART APEX II System	65
3.3.1	X-ray Source	68
3.3.2	K780 X-ray Generator	68
3.3.3	Timing Shutter and Collimator	68
3.3.4	APEX II CCD Detector	69
3.3.5	3-Axis SMART Goniometer	69
3.3.6	Video Camera	72
3.3.7	Radiation Safety Enclose with interlocks and Warning Lights	72
3.3.8	D8 Controller	72
3.3.9	Refrigerated Recirculator for the Detector	73
3.3.10	Computer	73
3.3.11	Accessories (low-temperature device)	73

3.4	Methodology	75
3.4.1	Crystal Selection and Orientation	78
3.4.2	Software	80
3.4.2.1	Data Collection and Data Reduction	80
3.4.2.2	Space Group Determination	81
3.4.2.3	Crystal Structure Solution	81
3.4.2.4	Structure Refinement	81
3.4.2.5	Absorption Correction	82
3.4.2.6	Crystal Structure Display	82
3.4.2.7	Preparation of Tables and Plot	83
3.5	Synthesis and Preparation of Crystals	84
3.5.1	1-(2,4-Dihydroxy-6-methoxyphenyl)-3-(4-methoxyphenyl)-propan-1-one	84
3.5.2	1-3-Dihydroxy-2-methyl-9,10-anthraquinone	84
3.5.3	12-(1,1-Dimethyl-2-propenyl)-5,9,10-trihydroxy-2,2-dimethyl-2 <i>H</i> , 6 <i>H</i> -pyrano[3,2- <i>b</i> ]xanthen-6-one	84
3.5.4	3,19-(2-Bromobenzylidene)andrographolide	85
3.5.5	3,19-(2,6-Dimethoxybenzylidene)andrographolide	85
<b>CHAPTER 4 RESULTS AND DISCUSSION</b>		
4.1	1-(2,4-Dihydroxy-6-methoxyphenyl)-3-(4-methoxyphenyl)propan-1-one	87
4.1.1	Data Collection and Refinement	87
4.1.2	Discussion	90
4.2	1-3-Dihydroxy-2-methyl-9,10-anthraquinone	95
4.2.1	Data Collection and Refinement	95
4.2.2	Discussion	98

4.3	12-(1,1-Dimethyl-2-propenyl)-5,9,10-trihydroxy-2,2-dimethyl-2 <i>H</i> , 6 <i>H</i> -pyrano[3,2- <i>b</i> ]xanthen-6-one	102
4.3.1	Data Collection and Refinement	102
4.3.2	Discussion	105
4.4	3,19-(2-Bromobenzylidene)andrographolide	110
4.4.1	Data Collection and Refinement	110
4.4.2	Discussion	113
4.5	3,19-(2,6-Dimethoxybenzylidene)andrographolide	118
4.5.1	Data Collection and Refinement	118
4.5.2	Discussion	121
<b>CHAPTER 5 CONCLUSION AND FURTHER RESEARCH</b>		
5.1	Conclusion	126
5.2	Further Research	129
<b>BIBLIOGRAPHY</b>		130
<b>Appendices</b>		
Appendix 1	Complete data for 1-(2,4-dihydroxy-6-methoxyphenyl)-3-(4-methoxyphenyl)-propan-1-one structure	134
Appendix 2	Complete data for 1-3-dihydroxy-2-methyl-9,10-anthraquinone structure	141
Appendix 3	Complete data for 12-(1,1-dimethyl-2-propenyl)-5,9,10-trihydroxy-2,2-dimethyl-2 <i>H</i> ,6 <i>H</i> -pyrano[3,2- <i>b</i> ]xanthen-6-one structure	145
Appendix 4	Complete data for 3,19-(2-bromobenzylidene)-andrographolide structure	151
Appendix 5	Complete data for 3,19-(2,6-dimethoxybenzylidene)andrographolide structure	158
<b>PUBLICATIONS LIST</b>		165



## LIST OF TABLES

	Page
 <b>CHAPTER 2</b>	
Table 2.1      Systematic Absences Condition	31
Table 2.2      Systematic Absences for Screw Axis	32
Table 2.3      Systematic Absences for Glide Planes	32
 <b>CHAPTER 4</b>	
Table 4.1      Crystal data and structure refinement for 1-(2,4-dihydroxy-6-methoxyphenyl)-3-(4- methoxyphenyl)propan-1-one	89
Table 4.2      Bond lengths (Å) and angles (°) for 1-(2,4-dihydroxy-6-methoxyphenyl)-3-(4- methoxyphenyl)propan-1-one	94
Table 4.3      Hydrogen-bond geometry, (Å, °)	95
Table 4.4      Crystal data and structure refinement for 1-3- dihydroxy-2-methyl-9,10-anthraquinone	97
Table 4.5      Bond lengths (Å) and angles (°) for 1-3-dihydroxy- 2-methyl-9,10-anthraquinone	101
Table 4.6      Hydrogen-bond geometry, (Å, °)	101
Table 4.7      Crystal data and structure refinement for 12- (1,1-dimethyl-2-propenyl)-5,9,10-trihydroxy-2,2- dimethyl-2 <i>H</i> ,6 <i>H</i> -pyrano[3,2- <i>b</i> ]xanthen-6-one	104
Table 4.8      Bond lengths (Å) and angles (°) for 12-(1,1- dimethyl-2-propenyl)-5,9,10-trihydroxy-2,2-dimethyl- 2 <i>H</i> ,6 <i>H</i> -pyrano[3,2- <i>b</i> ]xanthen-6-one	109
Table 4.9      Hydrogen-bond geometry, (Å, °)	110

Table 4.10	Crystal data and structure refinement for 3,19-(2-bromobenzylidene)andrographolide	112
Table 4.11	Bond lengths (Å) and angles (°) for 3,19-(2-bromobenzylidene)andrographolide	117
Table 4.12	Hydrogen-bond geometry, (Å, °)	118
Table 4.13	Crystal data and structure refinement for 3,19-(2,6-dimethoxybenzylidene)andrographolide	120
Table 4.14	Bond lengths (Å) and angles (°) for 3,19-(2,6-dimethoxybenzylidene)andrographolide	125
Table 4.15	Hydrogen-bond geometry, (Å, °)	125

## LIST OF FIGURES

	Page
<b>CHAPTER 1</b>	
Figure 1.1    Schematic representation of X-ray tube	3
Figure 1.2    Bragg's Law	6
Figure 1.3    Ewald sphere (radius $\frac{1}{\lambda}$ ) and limiting sphere (radius $\frac{2}{\lambda}$ )	9
<b>CHAPTER 2</b>	
Figure 2.1    Combination of two waves as vectors, $f_1 e^{i\varphi_1}$ and $f_2 e^{i\varphi_2}$ , on an Argand Diagram	20
Figure 2.2    Combination of N waves (N=6) on an Argand diagram; $\mathbf{F} = \sum_{j=1}^6 f_j e^{i\varphi_j}$	22
Figure 2.3    Atomic scattering factor: (a) stationary atom, $f_{j,\theta}$ (b) atom corrected for thermal vibration, $f_{j,\theta} T_{j,\theta}$	23
Figure 2.4    Structure factor $\mathbf{F}(hkl)$ plotted on an Argand diagram; $\varphi(hkl)$ is the resultant phase	26
Figure 2.5    Relationship between $\mathbf{F}(hkl)$ and $\mathbf{F}(\bar{h}\bar{k}\bar{l})$ leading to Friedel's law, from which $ \mathbf{F}(hkl)  =  \mathbf{F}(\bar{h}\bar{k}\bar{l}) $	30
Figure 2.6 $F(hkl)$ is the true structure factor of modulus $ F_0(hkl) $ and phase $\varphi(hkl)$	40
Figure. 2.7    Effect of sharpening on the radial decrease of the local average intensity $ \overline{\mathbf{F}_0} ^2$	42
Figure 2.8    Primary extinction: The phase changes on reflection at B and C are each $\pi/2$ , so that between the directions BE and CD there is a total phase difference of $\pi$ . Hence, some attenuation of the intensity occurs for the beam incident upon planes deeper in the crystal	53

Figure 2.9	“Mosaic” characters in a crystal: the angular misalignment between blocks may vary from 2’ to about 30’ of arc	54
Figure 2.10	Six membered rings conformation	61
Figure 2.11	Five membered rings conformation	62

### CHAPTER 3

Figure 3.1	The scheme of single crystal diffractometer system Bruker Apex II SMART CCD	67
Figure 3.2	SMART APEXII goniometer components	71
Figure 3.3	The gas flow circuit of the Cobra	74

### CHAPTER 4

Figure 4.1	The scheme of 1-(2,4-dihydroxy-6-methoxyphenyl)- 3-(4-methoxyphenyl)propan-1-one	90
Figure 4.2	The asymmetric unit of 1-(2,4-dihydroxy-6- methoxyphenyl)-3-(4-methoxyphenyl)propan-1-one, showing 50% probability displacement ellipsoids and the atomic numbering. Dashed lines indicate intramolecular O—H---O hydrogen bonds	92
Figure 4.3	The crystal packing of 1-(2,4-dihydroxy-6- methoxyphenyl)-3-(4-methoxyphenyl)propan-1-one, viewed down the <i>a</i> axis. Hydrogen bonds are shown as dashed lines	93
Figure 4.4	The scheme of 1-3-dihydroxy-2-methyl-9,10- anthraquinone	98
Figure 4.5	The structure of 1-3-dihydroxy-2-methyl-9,10- anthraquinone, showing 50% probability displacement ellipsoids and the atomic numbering. Intramolecular O—H---O and C—H---O hydrogen bonds are shown as dashed lines	99
Figure 4.6	The crystal packing of 1-3-dihydroxy-2-methyl-9,10- anthraquinone, viewed down the <i>b</i> axis. Hydrogen bonds are shown as dashed lines	100

Figure 4.7	The scheme of 12-(1,1-dimethyl-2-propenyl)-5,9,10-trihydroxy-2,2-dimethyl-2 <i>H</i> ,6 <i>H</i> -pyrano[3,2- <i>b</i> ]xanthen-6-one	105
Figure 4.8	The structure of 12-(1,1-dimethyl-2-propenyl)-5,9,10-trihydroxy-2,2-dimethyl-2 <i>H</i> ,6 <i>H</i> -pyrano[3,2- <i>b</i> ]xanthen-6-one, showing 50% probability displacement ellipsoids and the atomic numbering. The dashed lines indicate intramolecular O—H---O hydrogen bonds	107
Figure 4.9	The crystal packing of 12-(1,1-dimethyl-2-propenyl)-5,9,10-trihydroxy-2,2-dimethyl-2 <i>H</i> ,6 <i>H</i> -pyrano[3,2- <i>b</i> ]xanthen-6-one, viewed down the <i>c</i> axis. Hydrogen bonds are shown as dashed lines	108
Figure 4.10	The scheme of 3,19-(2-bromobenzylidene)-andrographolide	113
Figure 4.11	The structure of 3,19-(2-bromobenzylidene)-andrographolide, showing 50% probability displacement ellipsoids and the atomic numbering	115
Figure 4.12	The crystal packing of 3,19-(2-bromobenzylidene)-andrographolide, viewed down the <i>a</i> axis. Hydrogen bonds are shown as dashed lines	116
Figure 4.13	The scheme of 3,19-(2,6-dimethoxybenzylidene)-andrographolide	121
Figure 4.14	The structure of 3,19-(2,6-dimethoxybenzylidene)-andrographolide, showing 50% probability displacement ellipsoids and the atomic numbering. The dashed line indicates intramolecular C—H---O hydrogen bond	123
Figure 4.15	The crystal packing of 3,19-(2,6-dimethoxybenzylidene)-andrographolide, viewed approximately down the <i>b</i> axis. Hydrogen bonds are shown as dashed lines	124

## LIST OF PLATES

	Page
<b>CHAPTER 3</b>	
Plate 3.1     Single crystal diffractometer system Bruker Apex II SMART CCD	66
Plate 3.2     Goniometer	70
Plate 3.3     A 360° Phi Scan on a good quality crystal	76
Plate 3.4     Goniometer head	78
Plate 3.5     Crystal mounted on a glass fibre	78

## LIST OF ABBREVIATIONS

<b>CCD</b>	Charge-Coupled Device
<b>GooF</b>	Goodness of Fit
<b>ORTEP</b>	Oak Ridge Thermal Ellipsoid Plot
<b>R</b>	Reliability Index
<b>SADABS</b>	Siemens Area Detector Absorption Correction
<b>SAINT</b>	SAX Area-detector Integration (SAX-Siemens Analytical X-ray)
<b>SMART</b>	Siemens Molecular Analysis Research Tools
<b>TLC</b>	Thin Layer Chromatography
<b>wR</b>	Weighted Reliability Index

**KAJIAN STRUKTUR SINAR-X BEBERAPA PRODUK SEMULAJADI  
DARIPADA TUMBUH-TUMBUHAN *RAUWENHOFFIA SIAMENSIS* SCHEFF.,  
*PRISMATOMERIS MALAYANA* RIDL., *CRATOXYLUM FORMOSUM* SSP.  
*PRUNIFOLUM* AND *ANDROGRAPHIS PANICULATA* NEES**

**ABSTRAK**

Di dalam tesis ini kaedah kristalografi sinar-X hablur tunggal telah digunakan untuk menyelesaikan dan menentukan lima struktur produk semulajadi yang baru. Struktur molekul 1-(2,4-dihydroxy-6-methoxyphenyl)-3-(4-methoxyphenyl)propan-1-one,  $C_{17}H_{18}O_5$ , yang diasingkan dari *Rauwenhoffia siamensis* Scheff mempunyai dua molekul yang bebas secara kristalografinya dalam unit asimetrik. Sudut dihedral di antara dua gelang benzena adalah  $80.81 (7)^\circ$  dalam salah satu molekul dan  $65.89 (7)^\circ$  bagi molekul yang satu lagi. Molekul yang berhubungan secara simetri itu disambung melalui ikatan hidrogen intermolekul  $O-H\cdots O$  untuk membentuk rantai sepanjang arah [201]. Struktur ini terhablur dalam sistem monoklinik dengan kumpulan ruang  $P_{2_1/c}$ .

Struktur molekul 1-3-dihydroxy-2-methyl-9,10-anthraquinone,  $C_{15}H_{10}O_4$ , yang diasingkan dari akar *Prismatomeris malayana* Ridl., adalah planar. Ikatan hidrogen intramolekul  $O-H\cdots O$  dan  $C-H\cdots O$  dapat dilihat dalam struktur molekul. Molekul-molekul tersebut membentuk dimer yang berpusat simetri melalui ikatan hidrogen intermolekul  $O-H\cdots O$ . Struktur hablur ini



diperkukuhkan lagi oleh interaksi  $\pi-\pi$  yang lemah. Struktur ini terhablur dalam sistem monoklinik dengan kumpulan ruang  $P_{2_1/c}$ .

Bagi struktur 12-(1,1-dimethyl-2-propenyl)-5,9,10-trihydroxy-2,2-dimethyl-2*H*,6*H*-pyrano[3,2-*b*]xanthen-6-one,  $C_{23}H_{22}O_6$ , gelang xanthena dalam sistem ini adalah planar dan gelang kromena adalah dalam keadaan konformasi perahu berpintal. Kedudukan bagi bahagian 1,1-dimethyl-2-propenyl adalah sama satah dengan gelang yang tersambung. Terdapat ikatan intramolekul  $O-H\cdots O$  dalam struktur. Molekul-molekul tersebut membentuk dimer yang berpusat simetri melalui interaksi intermolekul  $C-H\cdots O$  yang lemah. Molekul-molekul bersambungan oleh ikatan hidrogen intermolekul  $O-H\cdots O$  untuk membentuk rantai satu dimensi sepanjang arah [010]. Struktur ini terhablur dalam sistem monoklinik dengan kumpulan ruang  $P_{2_1/c}$ .

Struktur 3,19-(2-bromobenzylidene)andrographolide,  $C_{27}H_{33}BrO_5$ , satu terbitan andrografolida, telah disepara sistesis dengan menggunakan andrografolida sebagai bahan permulaan. Struktur ini terdiri daripada cantuman tiga gelang segienam yang mempunyai konformasi kerusi dan gelang segilima yang mempunyai konformasi sampul. Kumpulan 2-bromofenil terkilas keluar dari gelang yang bersambung. Ikatan hidrogen  $O-H\cdots O$  dalam struktur membentuk rantai sepanjang paksi *b* yang berhubungan antara satu sama lain melalui interaksi  $C-H\cdots O$ . Struktur ini terhablur dalam sistem ortorombik dengan kumpulan ruang  $P_{2_12_12_1}$ .

Struktur 3,19-(2,6-dimethoxybenzylidene)andrographolide,  $C_{29}H_{38}O_7$ , satu analog andrografolida, telah disepara sistesis daripada andrografolida. Struktur ini terdiri daripada cantuman tiga gelang segienam yang mempunyai konformasi kerusi dan gelang segilima yang mempunyai konformasi berpintal. Ikatan hidrogen  $O-H\cdots O$  dalam struktur membentuk rantai sepanjang paksi  $a$  yang berhubungan antara satu sama lain melalui interaksi  $C-H\cdots \pi$ . Struktur ini terhablur dalam sistem ortorombik dengan kumpulan ruang  $P_{2_12_12_1}$ .

**X-RAY STRUCTURAL STUDIES OF SOME NATURAL PRODUCTS FROM  
*RAUWENHOFFIA SIAMENSIS* SCHEFF., *PRISMATOMERIS MALAYANA*  
RIDL., *CRATOXYLUM FORMOSUM* SSP. *PRUNIFOLUM* AND  
*ANDROGRAPHIS PANICULATA* NEES PLANTS**

**ABSTRACT**

In this thesis five new structures in the natural product compounds have been solved by single crystal X-ray crystallography method. The structure 1-(2,4-dihydroxy-6-methoxyphenyl)-3-(4-methoxyphenyl)propan-1-one,  $C_{17}H_{18}O_5$ , which was isolated from the leaves of *Rauwenhoffia siamensis* Scheff has two crystallographically independent molecules in the asymmetric unit. The dihedral angle between the two benzene rings is  $80.81 (7)^\circ$  in one molecule and  $65.89 (7)^\circ$  in the other. The symmetry related molecules are linked via O—H---O intermolecular hydrogen bonds to form chains along [201] direction. This structure crystallized in the monoclinic system with the space group  $P_{2_1/c}$ .

The structure of 1-3-dihydroxy-2-methyl-9,10-anthraquinone,  $C_{15}H_{10}O_4$ , which was isolated from the roots of *Prismatomeris malayana* Ridl., are coplanar. Intramolecular O—H---O and C—H---O hydrogen bonds can be observed in the molecular structure. The molecules form centrosymmetric hydrogen-bonded dimers via intermolecular O—H---O hydrogen bonds. The crystal structure is further stabilized by weak  $\pi-\pi$  interactions. This structure crystallized in the monoclinic system with the space group  $P_{2_1/c}$ .

For the structure of 12-(1,1-dimethyl-2-propenyl)-5,9,10-trihydroxy-2,2-dimethyl-2*H*,6*H*-pyrano[3,2-*b*]xanthen-6-one, C<sub>23</sub>H<sub>22</sub>O<sub>6</sub>, the xanthene ring system is essentially planar and the chromene ring is in a screw-boat conformation. The 1,1-dimethyl-2-propenyl substituent is coplanar with the attached ring. O—H---O intramolecular hydrogen bonds are observed in the structure. The molecules form centrosymmetric hydrogen-bonded dimers *via* weak intermolecular C—H---O interactions. The molecules are linked by intermolecular O—H---O hydrogen bonds to form a one-dimensional chain along [010] direction. This structure crystallized in the monoclinic system with space group  $P_{2_1/c}$ .

The structure of 3,19-(2-bromobenzylidene)andrographolide, C<sub>27</sub>H<sub>33</sub>BrO<sub>5</sub>, an andrographolide derivative, was semi-synthesized using andrographolide as a starting material. The structure contains three fused six-membered rings adopting chair conformations and a five-membered ring adopting an envelope conformation. The 2-bromophenyl group is twisted away from the attached ring. O—H---O hydrogen bonds in the structure form chains along the *b* axis which are interlinked *via* C—H---O interactions. This structure crystallized in the orthorhombic system with space group  $P_{2_12_12_1}$ .

The structure of 3,19-(2,6-dimethoxybenzylidene)andrographolide, C<sub>29</sub>H<sub>38</sub>O<sub>7</sub>, an andrographolide analogue, was semi-synthesized from andrographolide. The structure contains three fused six-membered rings adopting chair conformations and five-membered ring adopting a twisted conformation. Intermolecular O—H---O hydrogen bonds link the structure into

chains along the *a* axis which are interlinked *via* C—H--- $\pi$  interactions. This structure crystallized in the orthorhombic system with the space group  $P_{2_12_12_1}$ .

## **CHAPTER 1 INTRODUCTION**

### **1.1 Preliminary**

In this study, research on single crystal structure of natural products was carried out. This chapter describes basic X-ray crystallography theories and the characteristics of natural product.

### **1.2 X-ray Crystallography**

X-ray Crystallography is a study of crystal structure through X-ray diffraction techniques. We can examine the internal structure of crystals through X-ray diffraction pattern which can be interpreted mathematically by certain computer software written to deal with diffraction pattern. This leads to an understanding of the molecular and crystal structure of a substance. Crystals are three dimensional ordered structures that can be described as repetition of identical unit cells. The unit cell is characterized by six parameters, with 3 axial lengths ( $a, b, c$ ) and 3 interaxial angles ( $\alpha, \beta, \gamma$ ).

### **1.3 Generation of X-Ray**

X-rays are produced by accelerating electrons towards a metallic target, which is maintained at high positive potential difference,  $V$  relative to the cathode. These high-speed electrons strike the metallic target and rapidly decelerate. If enough energy is obtained, it is able to eject an electron from the inner shell of the metal atom and the electrons from higher energy levels will fill up the vacancy. This electronic transition causes the generation of X-ray (Figure 1.1).

The relation of the energy to the frequency of the X-ray radiation is through the Planck's constant,

$$E = h\nu \quad (1.1)$$

$E$  = Radiation energy

$h$  = Planck's constant

$\nu$  = frequency of the X-ray radiation

$$= \frac{c}{\lambda}, \text{ c = speed of light}$$

$\lambda$  = wavelength.

$$\text{So, } E = \frac{hc}{\lambda} \quad (1.2)$$

This indicates that the wavelength of radiation becomes smaller with larger energy transition.

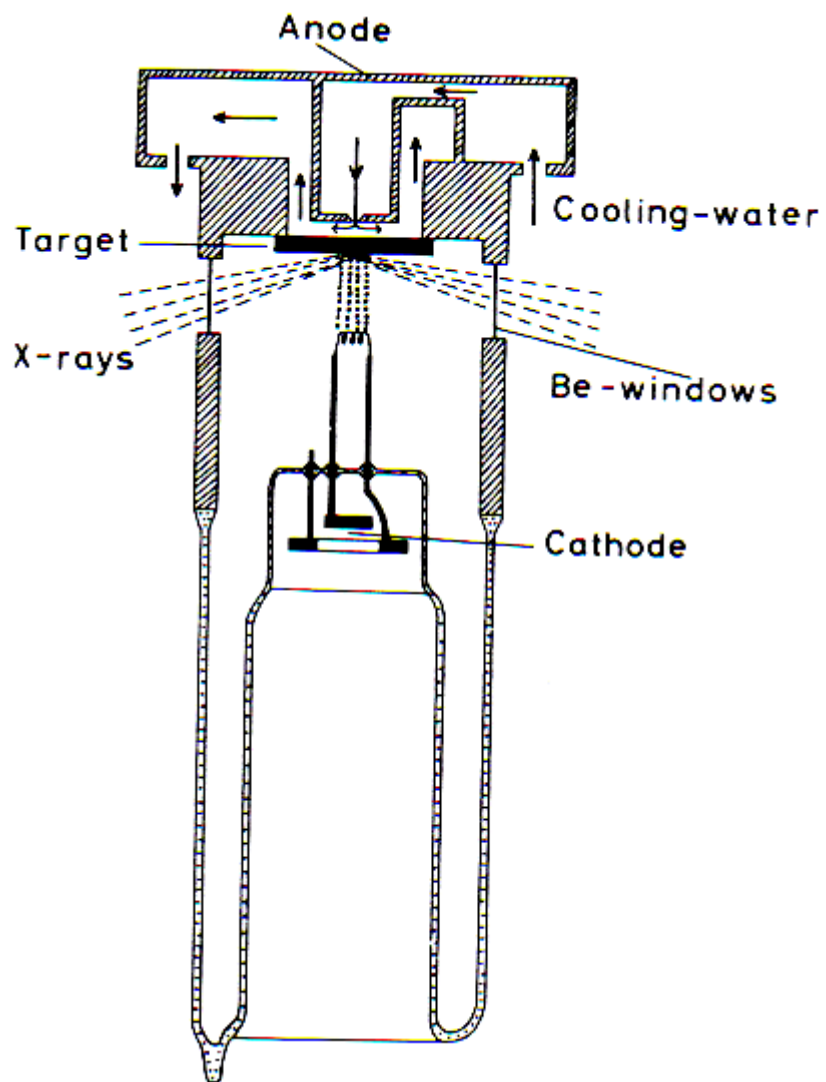


Figure 1.1 Schematic representation of X-ray tube (Luger, 1980).



## 1.4 X-ray Diffraction

Diffraction of an X-ray beam passing through a crystal occurs when the repeat distance in the crystal is about the same order of magnitude as the wavelength of the X-ray. The periodicity of crystal structures means that they can act as an X-ray diffraction grating. Crystals are used due to the diffraction pattern from one single molecule could be insignificant, but the many identical molecules in a crystal amplify the pattern.

X-ray beam generated from the X-ray tube contains not only the strong  $K_{\alpha}$  line but also the weaker  $K_{\beta}$  line and the continuous spectrum. A selective filter has an atomic number 1 or 2 less than the target metal is chosen to absorb the  $K_{\beta}$  component, with a relatively much smaller loss of  $K_{\alpha}$  (Stout & Jensen, 1989). In this single crystal X-ray structure determination research, a tunable graphite crystal monochromator is substituted for filter to select only the  $K_{\alpha}$  line ( $\lambda = 0.71073 \text{ \AA}$ ) emitted from the Mo X-ray source. The incident beam is then collimated by collimator system to produce a narrow beam (Bruker, 2005). The information about the lattice of a crystal is most easily obtained if the wavelength,  $\lambda$  is kept constant by using monochromatic X-ray. The monochromatic beam is then allowed to strike the crystal to be studied.

In 1912, Bragg noticed the similarity of diffraction to ordinary reflection (Stout & Jensen, 1989). By dealing the diffraction as reflection from plane in the lattice, he concluded a simple equation (Figure 1.2)

$$2d \sin\theta = n\lambda \quad (1.3)$$

$n$  = peak order

$\theta$  = angle between the incidence beam and the atomic planes

$\lambda$  = wavelength of X-ray

$d$  = interplanar spacing in the crystal lattice

This relation is known as Bragg's Law. For a known wavelength,  $\lambda$  and  $d$  spacing, the peak will occur at a particular  $\theta$  according to the peak order,  $n$ .

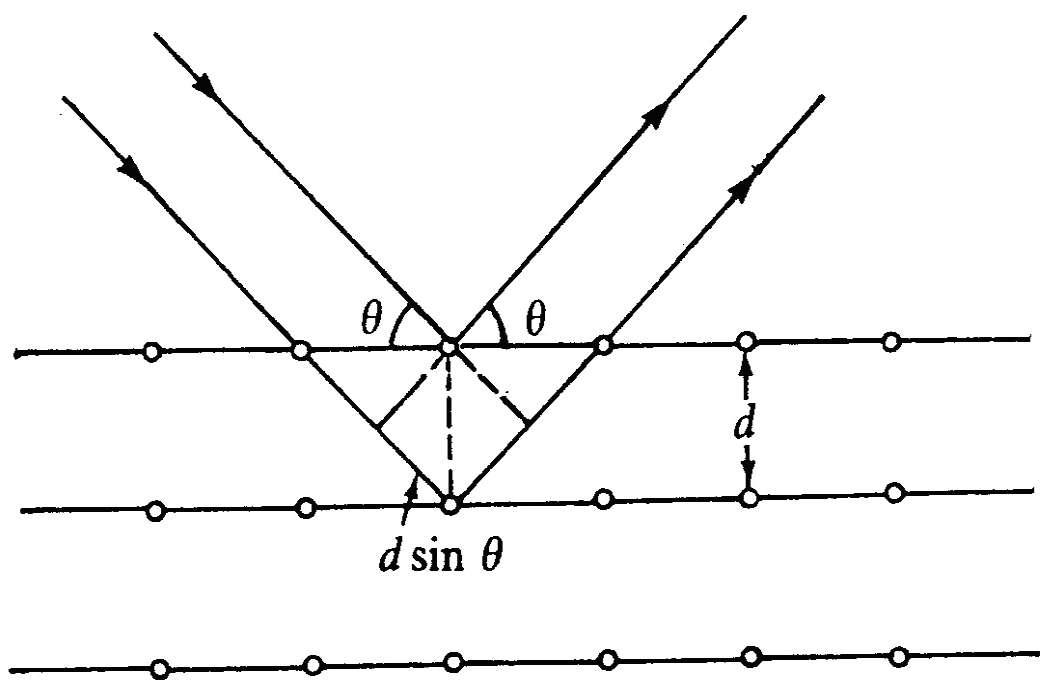


Figure 1.2 Bragg's Law (Halliday et al., 2001)

## 1.5 Reciprocal Lattice

From Bragg's law

$$\sin \theta = \frac{n\lambda}{2} \left( \frac{1}{d} \right) \quad (1.4)$$

$\sin \theta$  is inversely proportional to  $d$ . Interpretation of X-ray diffraction patterns would be facilitated if the inverse relation between  $\sin \theta$  and  $d$  could be replaced by a direct one by constructing a reciprocal lattice based on  $\frac{1}{d}$ , a quantity that varies directly as  $\sin \theta$  (Stout & Jensen, 1989).

The relation between the crystal lattice and the reciprocal lattice may be expressed in terms of vectors (Glusker & Trueblood, 1985).

$$\begin{aligned} \vec{a}^* &= \frac{\vec{b} \times \vec{c}}{\vec{a} \cdot \vec{b} \times \vec{c}} = \frac{\vec{b} \times \vec{c}}{V} \\ \vec{b}^* &= \frac{\vec{c} \times \vec{a}}{\vec{a} \cdot \vec{b} \times \vec{c}} = \frac{\vec{c} \times \vec{a}}{V} \\ \vec{c}^* &= \frac{\vec{a} \times \vec{b}}{\vec{a} \cdot \vec{b} \times \vec{c}} = \frac{\vec{a} \times \vec{b}}{V} \end{aligned} \quad (1.5)$$

$\vec{a}, \vec{b}, \vec{c}$  = unit vector in crystal lattice

$\vec{a}^*, \vec{b}^*, \vec{c}^*$  = unit vector in reciprocal lattice

For

$$V^* = \frac{1}{\vec{a} \cdot \vec{b} \times \vec{c}} = \frac{1}{V} \quad (1.6)$$

where  $V$  = volume in crystal lattice

$V^*$  = volume in reciprocal lattice

From equations (1.5) and (1.6), there is a translation between the vectors of the crystal lattice and the reciprocal lattice.  $\vec{a}^*$ ,  $\vec{b}^*$ ,  $\vec{c}^*$  are perpendicular to the  $bc$ ,  $ac$  and  $ab$  plane, respectively; likewise,  $\vec{a}^*$  is perpendicular to both  $\vec{b}$  and  $\vec{c}$ ,  $\vec{b}^*$  is perpendicular to both  $\vec{a}^*$  and  $\vec{c}^*$ , and so on (Glusker & Trueblood, 1985).

## 1.6 Ewald Sphere

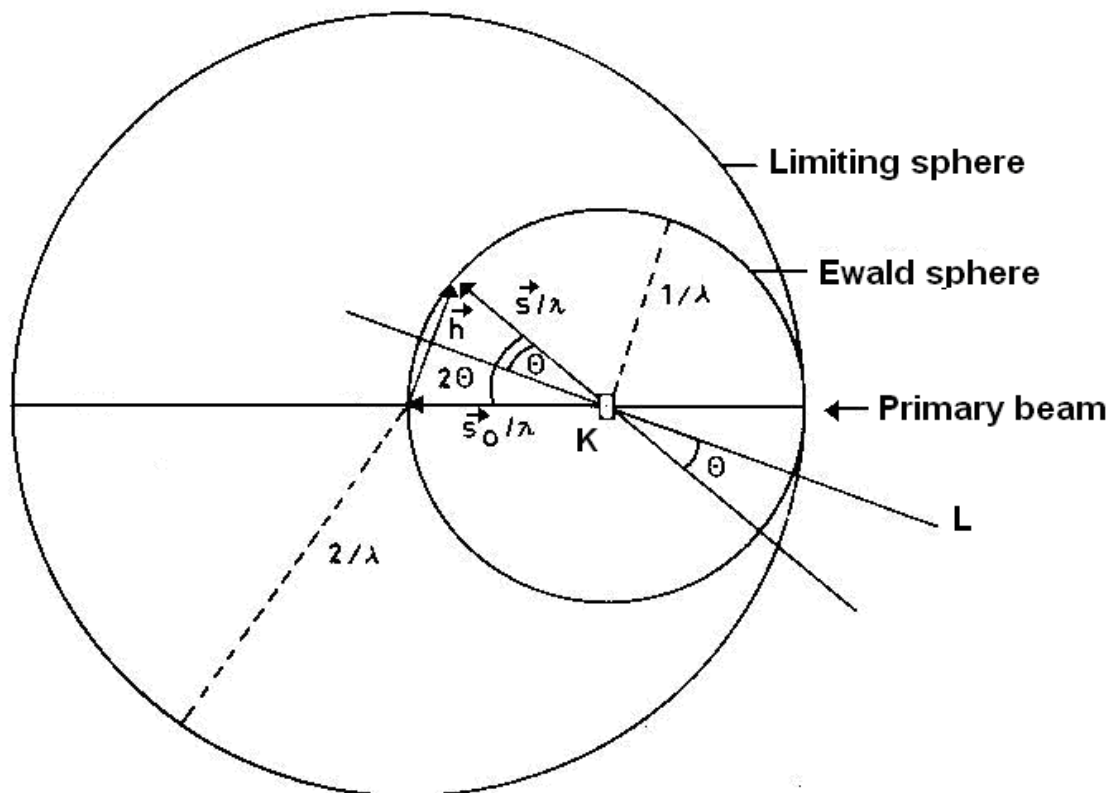


Figure 1.3 Ewald sphere (radius  $\frac{1}{\lambda}$ ) and limiting sphere (radius  $\frac{2}{\lambda}$ ) (Luger, 1980).

Paul Peter Ewald conceived Ewald's sphere, a sphere of radius  $\frac{1}{\lambda}$ , reciprocal lattice sphere. It is a geometric way that provides the condition for diffraction in reciprocal space. The sphere is centered on the crystal K and the origin of the reciprocal lattice lies in the transmitted beam, at the edge of the Ewald sphere. From the Ewald condition, consider a lattice plane L in a special position to cause diffraction (the diffraction position) where its normal vector h is on the surface of a sphere of radius  $\frac{1}{\lambda}$  around K.

$$\mathbf{h} = \frac{\mathbf{S} - \mathbf{S}_0}{\lambda} \quad (1.7)$$

where  $\mathbf{S}_0$  is the unit vector in the direction of the primary beam, and  $\mathbf{S}$  is the unit vector in the direction of the diffracted beam concerning a lattice plane with the normal vector  $\mathbf{h}$ .

When the reciprocal of the normal vector's magnitude,  $d$  satisfies the Bragg's Law, diffraction of a lattice plane, L, happens (Figure 1.3).

$$\frac{|\mathbf{h}|}{2} = \frac{1}{\lambda} \sin \theta, \quad d = \frac{1}{|\mathbf{h}|} \quad (1.8)$$

$$\therefore \lambda = 2d \sin \theta$$

Since the diameter of the sphere is  $\frac{2}{\lambda}$ , each reciprocal lattice point within that distance of the origin can be brought into coincidence with its surface.

For a given radiation with fixed wavelength,  $\lambda$  the number of possible reflections is limited and only those reflections in reciprocal space inside the sphere of radius  $\frac{2}{\lambda}$  can be observed. This sphere is called the “limiting sphere”. The limiting sphere has twice the radius of the Ewald sphere. Changing the wavelength of the incident radiation has the effect of enlarging (short  $\lambda$ ) or shrinking (longer  $\lambda$ ) the size of the sphere of reflection (Luger, 1980).

## **1.7 Natural Products**

Natural products play an important role in the development of drugs since ancient times. Typically, when a natural product is found to be active, it is chemically modified to improve its properties as a result of advances made in synthesis and separation method as well as in biochemical techniques. In this research, the single crystal samples of natural products are obtained from the Department of Chemistry, Faculty of Sciences, Prince of Songkla University, Songkhla, Thailand, the Department of Biomedical Sciences, Faculty of Medicine and Health Science, Universiti Putra Malaysia, Serdang, Malaysia and the Laboratory of Natural Products, Institute of Bioscience, Universiti Putra Malaysia, Serdang, Malaysia.



The samples were analysed using Bruker SMART APEX II CCD area detector diffractometer in the X-ray Crystallography Unit, School of Physics, Universiti Sains Malaysia, Penang, Malaysia. X-ray Crystallography technique is an ideal method to determine and identify the structure of compounds and was used in this research on natural products.

Natural products are compounds produced by living systems such as plants, animals and microorganisms. They have played a major role in the development of organic chemistry. The major chemical and physical methods of structure elucidation have been developed during the study of natural products (Hanson, 2003).

Thus, there have been important advances in the study of compounds from natural sources to identify the structures of the compounds physically and chemically. The development of diffraction technique, such as X-ray crystallography has greatly simplified the structure elucidation of natural products.

Naturally existing compounds may be divided into three categories (Hanson, 2003). Firstly, there are compounds which occur in all cells and play a central role in the metabolism and reproduction of those cells. These compounds include nucleic acids and common amino acids and sugars. They are known as primary metabolites. Secondly, the high-molecular-weight polymeric like cellulose, lignin and protein which form the cellular structures. Finally, there are compounds that are characteristic of a limited range of

species. They are secondary metabolites. Drugs are only obtained from pure and best behaviour derivation of secondary metabolite natural products.

In late 18<sup>th</sup> century, scientists turned the traditional medicine into modern medicine study. The active constituents were isolated from plant, were structurally characterized and then synthesized in the laboratories. This led to the development of various instruments for structural analysis such as chromatography methods (paper chromatography, thin layer chromatography (TLC), column chromatography, high performance liquid chromatography (HPLC), gas-liquid chromatography, ion exchange chromatography etc.). These chromatography methods are used for the analysis or separation of mixture existing in natural products and other compounds.

X-ray crystallography is an ideal method to determine the limited and small amount sample. The lattice structure, chemical formula, bond lengths and bond angles can be determined more accurately by using X-ray crystallography method. Thus, the molecular and crystal structures of the compounds of natural products can also be precisely determined using this technique.

#### **1.7.1 1-(2,4-Dihydroxy-6-methoxyphenyl)-3-(4-methoxyphenyl)propan-1-one**

*Rauwenhoffia siamensis* Scheff. belongs to the family of Annonaceae, which is widely distributed in Thailand, Malaysia and Indonesia. *R. siamensis* has a local Thai name, Nom Maew, and has been used for biofragrance (Chulalaksananukul et al., 1998). The compound 1-(2,4-dihydroxy-6-methoxyphenyl)-3-(4-methoxyphenyl)propan-1-one was isolated from the leaves of *R. siamensis*, which were collected from Songkhla province in the southern part of Thailand. The naringin dihydrochalcone which is derivative of compound 1-(2,4-dihydroxy-6-methoxyphenyl)-3-(4-methoxyphenyl)propan-1-one was known as a sweetener (Shin et al., 1995).

#### **1.7.2 1-3-Dihydroxy-2-methyl-9,10-anthraquinone**

*Prismatomeris malayana* Ridl. or "Kradook Kai" in Thai is a medicinal plant. The extract from the root of this plant has been used as folk medicine for the treatment of skin diseases (Perry, 1980). 1-3-dihydroxy-2-methylanthra-9,10-anthraquinone, has been isolated from the roots of *Prismatomeris malayana* Ridl. which were collected from the Phuket province in the southern part of Thailand. Rubiadin was isolated before from *Rubia cordifolia* (Tripathi et al., 1997) and *Hedyotis capitellata* (Ahmad et al., 2005). It possesses an antioxidant property which is better than that of EDTA, Tris, manitol, vitamin E and *p*-benzoquinone (Tripathi et al., 1997).

### 1.7.3 12-(1,1-Dimethyl-2-propenyl)-5,9,10-trihydroxy-2,2-dimethyl-2*H*,6*H*-pyrano[3,2-*b*]xanthen-6-one

Compound 12-(1,1-dimethyl-2-propenyl)-5,9,10-trihydroxy-2,2-dimethyl-2*H*,6*H*-pyrano[3,2-*b*]xanthen-6-one, macluraxanthone, was isolated from the bark of *Cratoxylum formosum* ssp. *prunifolium*, a shrub which was collected from Nhonkhai province in the north-eastern part of Thailand. It is part of our continuing search for bioactive compounds obtained from Thai medicinal plants (Chantrapomma et al., 2004; Chantrapomma, Boonnak et al., 2005; Chantrapomma, Fun et al., 2005; Boonnak et al., 2005; Fun et al., 2005; Boonsri et al., 2005). Compound 12-(1,1-dimethyl-2-propenyl)-5,9,10-trihydroxy-2,2-dimethyl-2*H*,6*H*-pyrano[3,2-*b*]xanthen-6-one has been reported previously (Monache et al., 1981; Menache et al., 1983; Goh et al., 1992), but its X-ray crystal structure has not yet been reported.

### 1.7.4 3,19-(2-Bromobenzylidene)andrographolide

*Andrographis paniculata* Nees (Acanthaceae) is one of the most important medicinal plants, having been used in Chinese Traditional and Indian Ayurvedic medicine for a wide range of illnesses. Extensive research on this plant extract and its constituents has revealed various pharmacological properties including anticancer and immunostimulatory activities (Kumar et al., 2004).

The active chemical constituents responsible for the pharmacological activities of *A. paniculata* are the labdane-type diterpene lactones, among which the major component is andrographolide. The stereochemistry of compound andrographolide has previously been established (Smith et al., 1982; Fujita et

al., 1984; Spek et al., 1987). Recent studies suggested that andrographolide is an interesting pharmacophore with anticancer and immunomodulatory activities and hence has the potential to be developed as a cancer chemotherapeutic agent (Stanslas et al., 2001; Rajagopal et al., 2003).

With the objective of developing andrographolide analogues with increased potency and good selectivity against human cancer cell lines, we subjected andrographolide to many semi-synthetic procedures yielding various structural analogues of this compound. Being one of the most promising anticancer andrographolide analogues, the compound of 3,19-(2-bromobenzylidene)andrographolide exhibited potency and better selectivity in NCI-USA cancer screening when compared with the parent compound of andrographolide. We have synthesized the compound of 3,19-(2-bromobenzylidene)andrographolide by reacting andrographolide with 2-bromobenzaldehyde at room temperature.

#### **1.7.5 3,19-(2,6-Dimethoxybenzylidene)andrographolide**

Andrographolide is a major component of labdane-type diterpene lactones isolated from *Andrographis paniculata* Nees. Previously, we have reported the crystal structure of 3,19-(2-bromobenzylidene)andrographolide (Ng et al., 2006), a lead antitumour agent of andrographolide analogues. In a subsequent study of derivatization of andrographolide, we have synthesized the compound of 3,19-(2,6-dimethoxybenzylidene)andrographolide, by reacting andrographolide with 2,6-dimethoxybenzaldehyde. These compounds were

synthesized with the aim of improving the antitumour potential of the parent compound andrographolide. Compound 3,19-(2,6-dimethoxybenzylidene)andrographolide was tested for cytotoxic activity in breast, lung and prostate cancer cell lines and it exhibited 50% inhibitory concentrations (IC<sub>50</sub>) in the submicromolar range. The X-ray crystal structure analysis of 3,19-(2,6-dimethoxybenzylidene)andrographolide was undertaken in order to establish its molecular structure and stereochemistry.

## **1.8 Objective**

The main objective of this research is to determine the molecular and crystal structure of the natural products. Through the X-ray structural analysis we will be provided with the information of the bond lengths, bond angles, conformation, coordination and other crystallographic information of the molecular structure of different natural product compounds. From this information we will know how the molecules are linked and the kind of bonding that attached them together in the crystal structure. From the crystal structure packing, we can see how the molecules are arranged in different planes.

After the process of data collection and structure determination, the results of the structure analysis through X-ray crystallography methods will enable biologists, chemists and pharmacists to find the active compounds that are potential candidates for developing useful drug usage as well as to help them in their work towards searching and developing better medicine in the future.

## **1.9 Thesis Overview**

In this thesis, the theory behind the X-ray structure analysis will be discussed in chapter 2. It is followed by explanations of the methods used in obtaining samples for analysis, data collection and data processing and structure determination. Chapter 4 will focus on the results of the data analysis and the interpretation of the structures determined. The conclusion of this study will be presented in chapter 5, which is the final chapter of the thesis. This final chapter will also include suggestions for future research.

## CHAPTER 2 X-RAY STRUCTURE ANALYSIS

There are two important expressions in crystal structure determination. One of these is the structure factor  $\mathbf{F}(hkl)$ , which is the amplitude of reflection from the set of  $(h,k,l)$  planes. The second expression is the electron density,  $\rho(xyz)$  as a Fourier series involving the structure factors.

### 2.1 Argand Diagram

The reflection of  $hkl$  consists of combined scattering waves by all atoms in the structure. The waves are represented as vectors with real and imaginary components, by an Argand diagram (Figure 2.1).

From Figure 2.1,

$$\mathbf{f}_1 = f_1 \cos \varphi_1 + i f_1 \sin \varphi_1 \quad (2.1)$$

$$\mathbf{f}_2 = f_2 \cos \varphi_2 + i f_2 \sin \varphi_2 \quad (2.2)$$



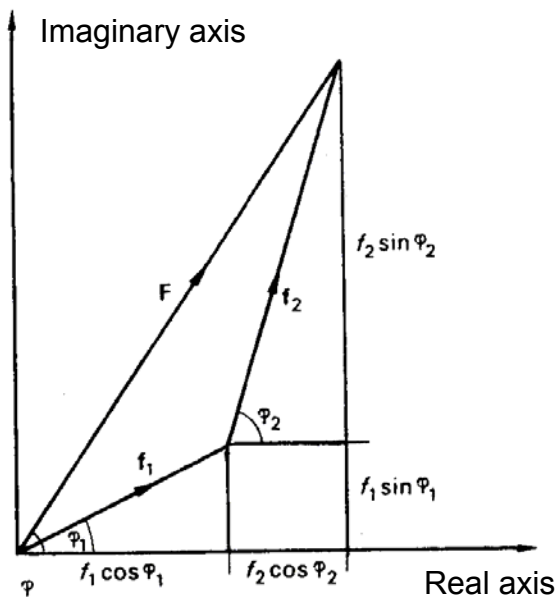


Figure 2.1 Combination of two waves as vectors,  $f_1 e^{i\varphi_1}$  and  $f_2 e^{i\varphi_2}$ , on an Argand diagram (Ladd & Palmer, 1979).

De Moivre's theorem states that

$$e^{\pm i\varphi} = \cos\varphi \pm i\sin\varphi \quad (2.3)$$

from equation (2.1) and (2.2)

$$f_1 = f_1 e^{i\varphi_1} \quad f_2 = f_2 e^{i\varphi_2} \quad (2.4)$$

Hence,

$$\mathbf{F} = f_1 e^{i\varphi_1} + f_2 e^{i\varphi_2} \quad (2.5)$$

## 2.2 Combination of N Waves

The combination of N waves, from (2.5)

$$\mathbf{F} = f_1 e^{i\varphi_1} + f_2 e^{i\varphi_2} + f_3 e^{i\varphi_3} + \dots + f_j e^{i\varphi_j} + \dots + f_N e^{i\varphi_N} \quad (2.6)$$

or

$$\mathbf{F} = \sum_{j=1}^N f_j e^{i\varphi_j} \quad (2.7)$$

In Figure 2.2, the equation 2.7 expresses a polygon of vectors. We can now derive  $\mathbf{F}$  as

$$\mathbf{F} = |\mathbf{F}| e^{i\varphi} \quad (2.8)$$

The conjugate of  $\mathbf{F}$  is  $\mathbf{F}^*$

$$\mathbf{F}^* = |\mathbf{F}| e^{-i\varphi} \quad (2.9)$$

Hence, the amplitude  $|\mathbf{F}|$  is given by

$$|\mathbf{F}|^2 = \mathbf{F} \mathbf{F}^* \quad (2.10)$$

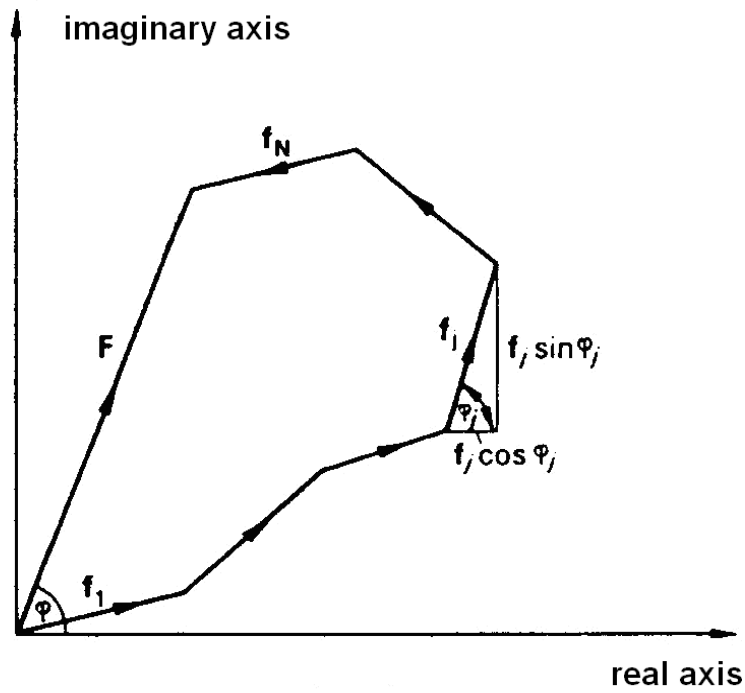


Figure 2.2 Combination of N waves (N=6) on an Argand digram;  
 $\mathbf{F} = \sum_{j=1}^6 f_j e^{i\phi_j}$  (Ladd and Palmer, 1979).

### 2.3 Phase Difference

The expression of phase in terms of the positions of the atoms and the indices of the reflection is needed before the structure factor can be calculated. There is a phase differences of one cycle ( $2\pi$  radian or  $360^\circ$ ) between reflections from any set of  $(h,k,l)$  planes. The path difference associated with waves scattered by an atom  $j$  whose position relative to the origin is specified by the coordinates  $x_j, y_j, z_j$  is given as (Ladd and Palmer, 1979),

$$\delta_j = \lambda (hx_j + ky_j + lz_j) \quad (2.11)$$

The corresponding phase difference (angular measure) is given by

$$\phi_j = (2\pi/\lambda) \delta_j$$

or 
$$\phi_j = 2\pi (hx_j + ky_j + lz_j) \quad (2.12)$$

## 2.4 The Atomic Scattering Factor

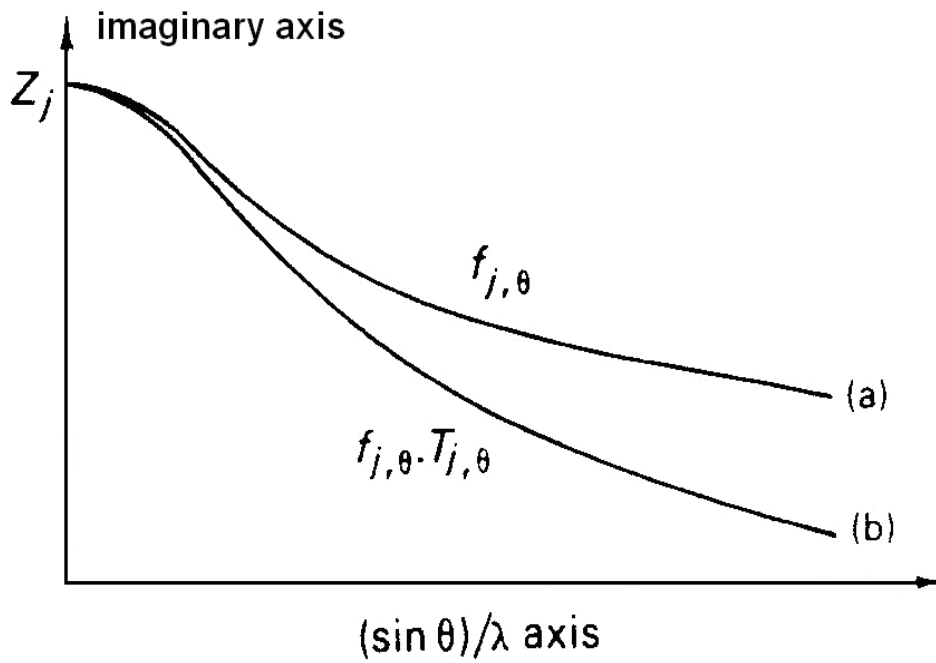


Figure 2.3 Atomic scattering factor:  
 (a) stationary atom,  $f_{j,\theta}$   
 (b) atom corrected for thermal vibration,  $f_{j,\theta} T_{j,\theta}$   
 (Ladd & Palmer, 1979).

The amplitudes of the waves scattered by atoms, the atomic scattering factors,  $f_j$ , is required to evaluate the combined scattering from the atoms in the unit cell. The atomic scattering factor depends upon the nature of the atom, the direction of scattering, the wavelength of X-rays used, and the thermal vibration of the atom (Ladd & Palmer, 1979). Initially,  $f_j$  is based upon the number of extranuclear of electrons in the atom. The atomic number of the  $j$ th atomic species,  $Z_j$  is its maximum value for a given atom  $j$ .  $f_j$  has its maximum value on the direction of the incident beam where  $\sin\theta(hkl) = 0$ .

$$f_{j,\theta(\theta=0)} = Z_j \quad (2.13)$$

$f$  is measured in number of electrons.

Assumed isotropic vibration, where the temperature factor correction for atom  $j$  is

$$T_{j,\theta} = \exp[-B_j(\sin^2\theta)/\lambda^2] \quad (2.14)$$

$B_j$  is the temperature factor of atom  $j$ , and is given as

$$B_j = 8\pi^2 \overline{U_j^2} \quad (2.15)$$

$\overline{U_j^2}$ , which is a function of temperature, is the mean square amplitude of vibration of atom  $j$  from its equilibrium position in a direction normal to the